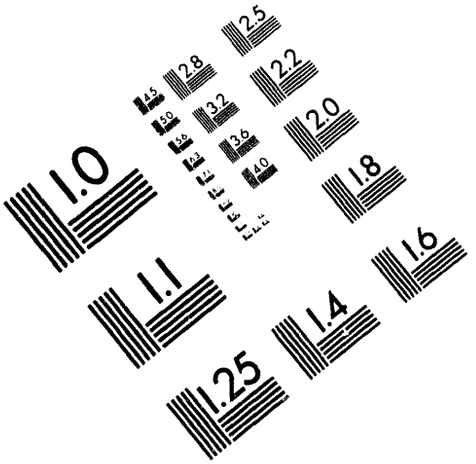

Association for Information and Image Management

1100 Wayne Avenue, Suite 1100
Silver Spring, Maryland 20910

301/587-8202

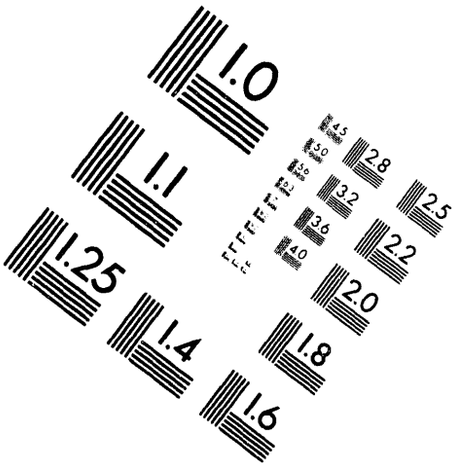

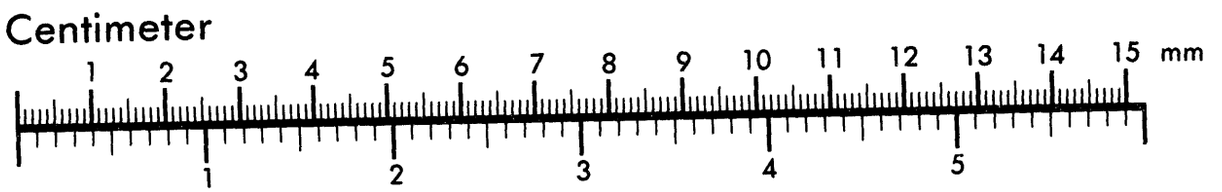

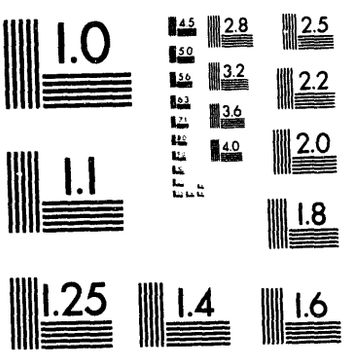

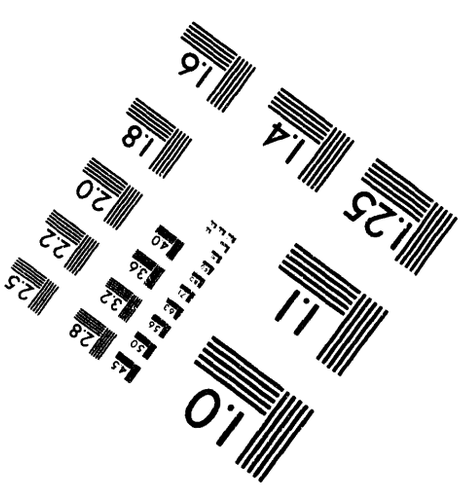

MANUFACTURED TO AIIM STANDARDS
BY APPLIED IMAGE, INC.

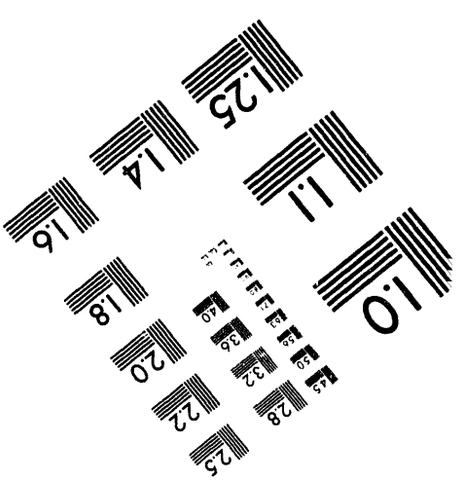

1 of 1

LBL-35590
UC-414

To be published in the Proceedings of the
Tenth Winter Workshop on Nuclear Dynamics
Snowbird, Utah, 15-21 January 1994,
World Scientific Publishing Co.

Collective Flow in Au+Au Collisions

Hans-Georg Ritter
Lawrence Berkeley Laboratory
University of California, Berkeley, CA 94720

and

The EOS Collaboration

May 1994

This work was supported by the Director, Office of Energy Research, Division of Nuclear Physics of the Office of High Energy and Nuclear Physics of the U.S. Department of Energy under Contract DE-AC03-76SF00098

COLLECTIVE FLOW IN AU+AU COLLISIONS

H. G. Ritter[1] for the EOS Collaboration:

S. Albergo[6], F. Bieser[1], F. P. Brady[4], Z. Caccia[6], D. A. Cebra[4], A. D. Chacon[5], J. L. Chance[4], Y. Choi[3], S. Costa[6], J. Elliott[3], M. Gilkes[3], J. A. Hauger[3], A. Hirsch[3], E. L. Hjort[3], A. Insolia[6], M. Justice[2], D. Keane[2], V. Lindenstruth[7], H. S. Matis[1], M. McMahan[1], C. McParland[1], W. F. J. Mueller[7], D. L. Olson[1], M. Partlan[4], N. Porile[3], R. Potenza[6], G. Rai[1], J. Rasmussen[1], J. Romanski[6], J. L. Romero[4], G. V. Russo[6], H. Sann[7], R. Scharenberg[3], A. Scott[2], Y. Shao[2], B. Srivastava[3], T. J. M. Symons[1], M. Tincknell[3], C. Tuvè[6], S. Wang[2], P. Warren[3], D. Weerasundara[2], H. H. Wieman[1], and K. L. Wolf[5]

[1] *Lawrence Berkeley Laboratory, Berkeley, California 94720*
[2] *Kent State University, Kent, Ohio 44242*
[3] *Purdue University, West Lafayette, Indiana 47907*
[4] *University of California, Davis, California 95616*
[5] *Texas A&M University, College Station, Texas 77843*
[6] *Università di Catania and INFN-Sezione di Catania, 95129 Catania, Italy*
[7] *Gesellschaft für Schwerionenforschung, D-64220 Darmstadt 11, Germany*

ABSTRACT

Based on a preliminary sample of Au + Au collisions in the EOS time projection chamber at the Bevalac, we study sideward flow as a function of bombarding energy between 0.25A GeV and 1.2A GeV. We focus on the increase in in-plane transverse momentum per nucleon with fragment mass. We also find event shapes to be close to spherical in the most central collisions, independent of bombarding energy and fragment mass up to ^{4}He.

1. Introduction

Collective effects have played an important role in the study of nuclear collisions. As far back as the 1950s, hydrodynamic models have been used to predict various kinds of collective behavior.[1] For non-zero impact parameters, the predominant fluid dynamic effect is a sideward deflection of the participant matter in the reaction plane. Such collective correlations, caused by the release of compressional energy, provide a measure of the nuclear pressure generated in the collision. Models indicate that collective correlations are established during the early, high density stage of the collision. They are minimally distorted during the subsequent expansion process. Thus,

fluid-like correlations are regarded as being among the most appropriate observables for studying the equation of state of the compressed nuclear matter.

Experiments with large solid angle acceptance detectors have confirmed the existence of collective correlations, and have provided measurements of many aspects of the phenomenon. The EOS Time Projection Chamber is a new 4π detector which was designed to continue the progress made during the earlier phases of the Bevalac program. It offers a simple and seamless acceptance, good particle identification, and adequate statistics for a comprehensive characterization of the relevant physics. In these proceedings, we report flow results from preliminary EOS data and preliminary data on event shapes in very central collisions of Au + Au.

2. The EOS Detector

The EOS Time Projection Chamber has a rectangular geometry, and operates in a 1.3 T dipole field provided by a superconducting magnet at the Bevalac's Heavy Ion Spectrometer System (HISS) facility. Unlike previous TPCs, EOS relies solely on pads for readout. The pad plane covers an area of 1.54×0.96 m^2, with 128 pad rows along the longer dimension, and 120 pads per row. Details about the chamber, the electronics and the data acquisition have been reported previously.[2] The standard EOS detector configuration includes the TPC, a multiple sampling ionization chamber (MUSIC II) positioned to intercept projectile spectator fragments, an array of scintillator slats to provide time-of-flight information at small polar angles, and a high efficiency neutron detector (MUFFINS). Only data from the TPC have been used in the current analysis.

3. In-plane Transverse Momentum

Our initial investigation of collective effects in Au + Au collisions includes the same in-plane transverse momentum analysis with essentially the same data selection criteria as used by the Plastic Ball group.[3] In particular, all nuclear fragment species up to ^{4}He are included, and we select an interval of multiplicity centered about the value where the flow has its maximum. The transverse momentum method[4] has been used to calculate the quantity $\langle p^x(y')/A \rangle$, the mean transverse momentum per nucleon in the reaction plane.

Fig. 1 presents $\langle p^x(y')/A \rangle$ as a function of the normalized rapidity y' for each of the six bombarding energies under investigation. We observe the classic "S"-shaped curve which changes sign at $y' = 0$. Although projectile-target symmetry dictates $p^x(y') = -p^x(-y')$, even an ideal 4π detector cannot satisfy this condition because absorption and energy loss in the target introduce distortions for y' approaching -1. In the EOS detector, the target was located about 14 cm upstream from the active volume of the TPC, leading to optimized performance near mid-rapidity and above, at the expense of a progressive loss of acceptance approaching target rapidity. At each beam energy, we fit the $\langle p^x(y')/A \rangle$ curves over the region indicated by the solid lines

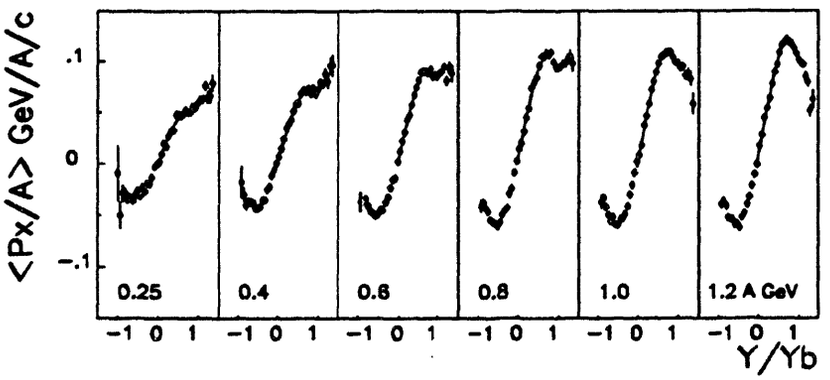

Fig. 1: Transverse momentum per nucleon projected on the reaction plane, as a function of normalized rapidity, for Au + Au collisions at six beam energies.

in Fig. 1 with a function of the form $my' - m_3y'^3$; the fitted values of m characterize the overall magnitude of the sideward flow effect among participant fragments, and these slopes are known simply as "flow" in the literature.

All fragment species up to ^{4}He were included when computing the results. In this work, we focus on the dependence of collective effects on fragment mass, and Fig. 2 presents preliminary flow excitation functions separately for protons, deuterons and alphas. The measurements in Fig. 2 show a consistent pattern of increase in sideward flow per nucleon with increasing fragment mass number A. Such an increase was previously reported by the Plastic Ball group[5] for collisions of Au + Au at a beam energy of 200A MeV. Fig. 2 also confirms the previously observed increase in flow with beam energy.

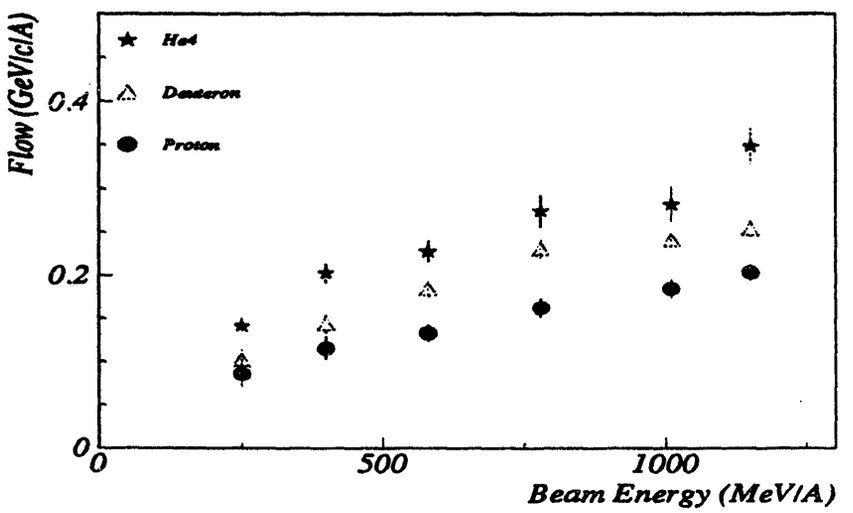

Fig. 2: Flow excitation function for protons, deuterons and alphas from Au + Au collisions.

4. Orthogonal Components of Sideward Flow

The observed transverse momentum $\mathbf{p}^{\perp}$ of a fragment has an uncorrelated ($\mathbf{p}^{\perp}_{uncor}$) and a correlated ($\mathbf{p}^{\perp}_{cor}$) component. $\mathbf{p}^{\perp}_{cor}$ is an effect of directed flow. We can approximate $\mathbf{p}^{\perp}_{uncor}$ using mixed events, *i.e.*, events generated by randomly selecting M tracks, each from a different observed event with multiplicity M. The correlated motion can be decomposed into two orthogonal parts: the azimuthal component, associated with rotations of $\mathbf{p}^{\perp}$ relative to an uncorrelated distribution, and the radial component of sideward flow, associated with changes in the magnitude of $\mathbf{p}^{\perp}$ relative to an uncorrelated distribution. Measurements of these two components complement each other, and together, they place more complete and stringent constraints on dynamical models. Radial flow, however, can not be distinguished by this method and would be treated as part of the uncorrelated motion.

The azimuthal pair correlation function[6] makes use of the variable ψ, the smaller angle between the transverse momenta of two fragments, and is defined as

$$C(\psi) = \frac{P_{cor}(\psi)}{P_{uncor}(\psi)}, \tag{1}$$

where $P_{cor}(\psi)$ is the ψ distribution for observed pairs and $P_{uncor}(\psi)$ is the ψ distribution for pairs from mixed events. Sideward flow leads to an enhanced probability for fragments to be emitted with azimuths close to each other, near the reaction plane orientation; thus, if $C(\psi)$ is plotted for a rapidity interval that is not centered on mid-rapidity, we observe $C(\psi) > 1$ at small ψ and $C(\psi) < 1$ at large ψ. If fragments within a given rapidity interval are distributed in azimuthal angle φ according to $P(\varphi) \propto 1 + \lambda \cos\varphi$, then $C(\psi) = 1 + 0.5\lambda^2 \cos\psi$ (see Ref. 6). Fitted λ values provide a dimensionless measure of the azimuthal flow component. The azimuthal pair correlation function offers several advantages over previous flow analyses: it circumvents the need for event-by-event estimates of the reaction plane and the need to correct for dispersion in these estimates, it allows flow measurements in different rapidity intervals to be completely independent of each other, and the denominator in $C(\psi)$ automatically corrects for any azimuthal asymmetry introduced by the detector. Only forward rapidities are studied in the current analysis.

To characterize the radial component of sideward flow, we introduce a new quantity which we call the radial pair variance function:

$$\sigma^2(\psi) = \langle p^2_{sum}(\psi)\rangle - \langle p_{sum}(\psi)\rangle^2, \tag{2}$$

where $p_{sum} = p_i^{\perp}/A_i + p_j^{\perp}/A_j$ is the sum of the $\mathbf{p}^{\perp}$ magnitudes per nucleon for the pair. In this case there is no reason to compute a ratio like P_{cor}/P_{uncor}, because $\sigma^2(\psi)$ is flat for mixed events. The fact that $\mathbf{p}^{\perp}$ magnitudes tend to be larger when a fragment's azimuth is parallel to the flow direction, and tend to be smaller when antiparallel, leads to an inequality $\sigma^2(\psi \sim 0^{\circ}) > \sigma^2(\psi \sim 180^{\circ})$. σ^2 decreases linearly with increasing ψ. This can be demonstrated analytically for an idealized example

where there are no thermal fluctuation in $\mathbf{p}^{\perp}$, and simulations with realistic momenta also indicate linear $\sigma^2(\psi)$. To characterize the magnitude of the radial component of sideward flow in momentum units, we define $S = \sqrt{(d\sigma^2/d\psi)}$.

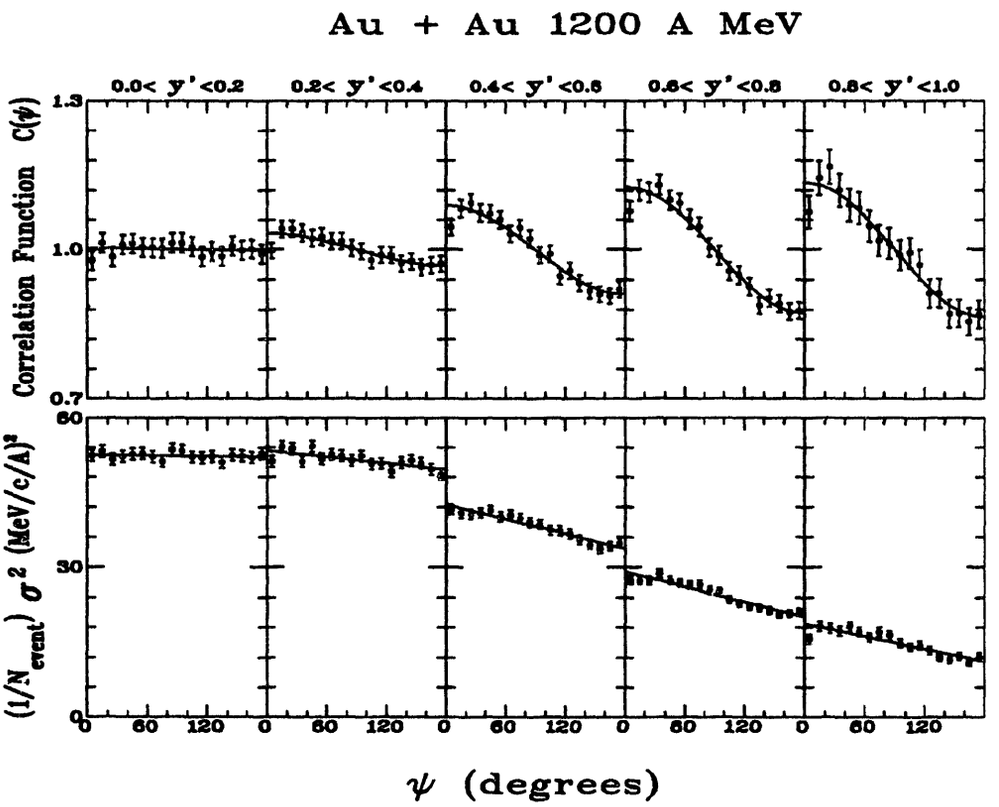

Fig. 3: Azimuthal pair correlation functions and radial pair variance functions in five rapidity intervals spanning mid-rapidity to projectile rapidity, for Au + Au at 1.2A GeV.

Fig. 3 shows azimuthal pair correlation functions $C(\psi)$ and radial pair variance functions $\sigma^2(\psi)$ in five rapidity intervals spanning mid-rapidity to projectile rapidity, for Au + Au at 1.2A GeV. The solid curves in the $C(\psi)$ panels represent least-squares fits using the function $1+0.5\lambda^2 \cos\psi$, and the $\sigma^2(\psi)$ data in the lower panels are fitted using a straight line. In this analysis of azimuthal and radial components of sideward flow, only protons and deuterons from events with $M > 0.4M^{max}$ have been included.

5. Dependence of Components of Sideward Flow on Fragment Mass

In order to investigate the fragment mass dependence, we have sorted protons and deuterons into separate samples and computed the same quantities as plotted in Fig. 3. The system Au + Au at 1.2A GeV currently provides the best data on fragment flow, but still does not yield useful same-fragment pair correlation statistics for $A \geq 3$. Fig. 4 shows the fitted sideward flow components λ and S for our standard rapidity intervals. At all of the rapidities studied, the observed pattern is consistent

with a simple coalescence picture:[7] the radial component of sideward flow S is the same for p and d, while $\lambda_d = 2\lambda_p$ within experimental uncertainties.

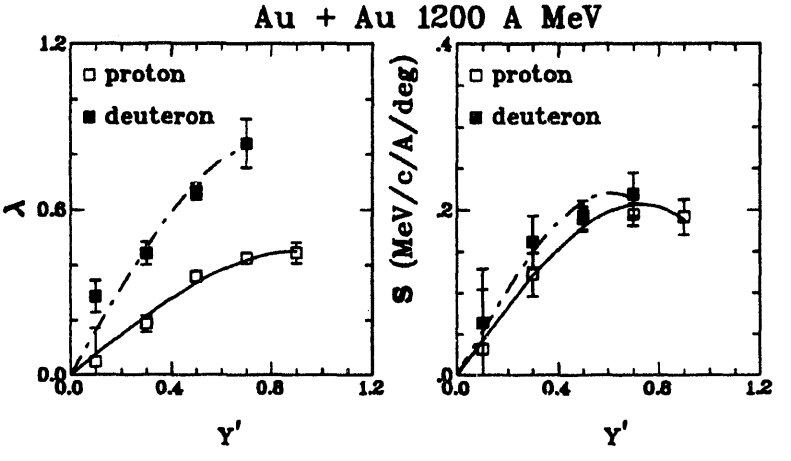

Fig. 4: Azimuthal flow component $\lambda(y')$ and radial component of sideward flow $S(y')$ separately evaluated for protons and deuterons from collisions of $1.2A$ GeV Au + Au.

An important advantage of the EOS TPC is its seamless acceptance, which is simple enough to be simulated with good accuracy. To estimate the effect of detector distortion on the observables under investigation, we use events from a version of the *FREESCO* statistical event generator[8] to which a phenomenological flow correlation[9] has been added. The simulations indicate that any detector-related distortion of the measured sideward flow components is not larger than the statistical uncertainty in samples of several thousand events.

6. Event Shapes in Central Collisions

The energy contained in directed flow is only a few percent of the total available kinetic energy.[3,10] From entropy considerations[11] and from general energy estimates,[12] we would expect to see a much larger fraction of the total energy contained in collective flow. From a systematic study of intermediate mass fragments the FOPI collaboration has obtained evidence for a large amount of "radial" flow.[13,10] The analysis has been done with the most violent events with very stringent cuts on centrality and within a limited range of emission angle in the center of mass system. Therefore, it is not possible to distinguish experimentally between radial (isotropic) flow and azimuthally symmetric flow perpendicular to the beam axis, the limiting case of directed flow for very central events. The EOS data for $y' > 0$ are well-suited for testing event shapes and elucidating these issues.

The thermalization ratio $R = 2\sum |\mathrm{p}^{\perp}| \;/\; \pi \sum |p^z_{cm}|$ has been widely used since the time when the first 4π measurements became available. An isotropic source implies $R = 1$ and measurements of R can provide information about event shapes. However, directed collective flow effects, kinematic cuts, and detector distortions

make the interpretation of R complicated. The presence of spectator matter can bias the thermalization ratio R towards lower values. In order to avoid the possibility of such bias, we include only fragments which satisfy $p_b/A > 0.27$ GeV/c, where p_b denotes fragment momentum transformed into the rest frame of the projectile. This cut biases R in the opposite direction, but it is relatively easy to correct this bias by using simulated events from the *FREESCO* event generator[8] with the same cut.

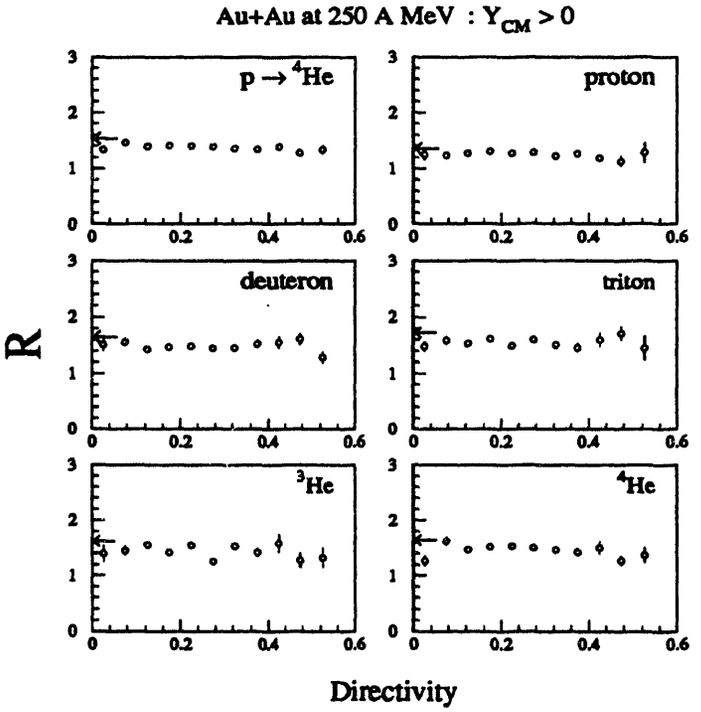

Fig. 5: Average thermalization ratio R versus directivity D for different light fragment species from $0.25A$ GeV Au + Au events with more than 30 detected baryonic fragments at forward rapidities ($y' > 0$). Note that R values in the vicinity of the horizontal arrow are consistent with a spherical event shape.

As a measure for the centrality of the collision, we use the directivity variable[14] $\mathbf{D} = \sum \mathbf{p}^{\perp} \; / \; \sum |\mathbf{p}^{\perp}|$. Fig. 5 presents average thermalization ratios R in bins of directivity magnitude D, for different light fragment species from $0.25A$ GeV Au + Au events with more than 30 detected baryonic fragments at $y' > 0$. Results for the other beam energies show similar behavior. The arrows on the vertical scales mark the R values for an isotropic source with the same spectator cut ($p_b/A > 0.27$ GeV/c) as applied to the EOS data. The main conclusion based on these preliminary data is that the most central collisions (lowest D) are consistent with being close to spherical in shape for all light fragment species at all beam energies studied. Thus, we would expect that the flow observed in the FOPI data is spherically symmetric radial flow, predicted a long time ago.[15] It should be seen at all impact parameters

and it should agree well with model calculations[16] that reproduce the directed flow since it is generated by the same mechanism.

This work was supported by the Director, Office of Energy Research, Office of High Energy and Nuclear Physics, Division of Nuclear Physics of the U.S. Department of Energy under Contract DE-AC03-76SF00098.

7. References

[1] S.Z. Belen'kji and L.D. Landau, Nuovo Cimento, **1**, 15 (1956); G.F. Chapline, M.H. Johnson, E. Teller, and M.C. Weiss, Phys. Rev. D **8**, 4302 (1973); W. Scheid, H. Müller, and W. Greiner, Phys. Rev. Lett. **32**, 741 (1974).

[2] G. Rai, A. Arthur, F. Bieser, C.W. Harnden, R. Jones, S. Kleinfelder, K. Lee, H.S. Matis, M. Nakamura, C. McParland, D. Nesbitt, G. Odyniec, D. Olson, H.G. Pugh, H.G. Ritter, T.J.M. Symons, H. Wieman, M. Wright, R. Wright, and A. Rudge, IEEE Trans. Nucl. Sci. **37**, 56 (1990).

[3] K.G.R. Doss, H.-Å. Gustafsson, H.H. Gutbrod, K.H. Kampert, B. Kolb, H. Löhner, B. Ludewigt, A.M. Poskanzer, H.G. Ritter, H.R. Schmidt, and H. Wieman, Phys. Rev. Lett. **57**, 302 (1986); H.H. Gutbrod, A.M. Poskanzer, and H.G. Ritter, Rep. Prog. Phys. **52**, 1267 (1989).

[4] P. Danielewicz and G. Odyniec, Phys. Lett. **157B**, 146 (1985).

[5] K.G.R. Doss, H.-Å. Gustafsson, H.H. Gutbrod, J.W. Harris, B.V. Jacak, K.-H. Kampert, B. Kolb, A.M. Poskanzer, H.G. Ritter, H.R. Schmidt, L. Teitelbaum, M. Tincknell, S. Weiss, and H. Wieman, Phys. Rev. Lett. **59**, 2720 (1987).

[6] S. Wang, Y.Z. Jiang, Y.M. Liu, D. Keane, D. Beavis, S.Y. Chu, S.Y. Fung, M. Vient, C. Hartnack, and H. Stöcker, Phys. Rev. C **44**, 1091 (1991).

[7] Y. Shao, Ph.D. thesis, Kent State U. (1994).

[8] G. Fai and J. Randrup, Nucl. Phys. **A404**, 551 (1983); Comp. Phys. Comm. **42**, 385 (1986).

[9] A.F. Barghouty, G. Fai, and D. Keane, Nucl. Phys. **A535**, 715 (1991).

[10] T. Wienold *et al.,* these proceedings.

[11] K.G.R. Doss, H.A. Gustafsson, H.H. Gutbrod, B. Kolb, H. Löhner, B. Ludewigt, A.M. Poskanzer, T. Renner, H. Riedesel, H.G. Ritter, A. Warwick, and H. Wieman, Phys. Rev. C **32**, 116 (1985).

[12] R. Stock, Phys. Rep. **135**, 259 (1986).

[13] S.C. Jeong *et al.,* GSI Preprint 93-38.

[14] J.P. Alard *et al.,* Phys. Rev. Lett. **69**, 889 (1992);

[15] P.J. Siemens and J.O. Rasmussen, Phys. Rev. Lett. **42**, 880 (1979).

[16] P. Danielewicz and Q. Pan, Phys. Rev. C **46**, 2002 (1993).

DATE
FILMED
10/14/94
END